Progress In Electromagnetics Research C, Vol. 54, 75–84, 2014

A T-Section Dual-Band Matching Network for Frequency-Dependent Complex Loads Incorporating Coupled Line with DC-Block Property Suitable for Dual-Band Transistor Amplifiers

Mohammad A. Maktoomi[1, *], Mohammad S. Hashmi[1, 2], and Fadhel M. Ghannouchi[2]

Abstract—This paper reports design of a new dual-band T-type impedance transformer also exhibiting DC-blocking feature. The design aims at achieving matching for frequency-dependent complex loads having distinct values at two arbitrary frequencies to Z_s (here, $50\,\Omega$). A step-wise analysis on the developed dual-band impedance transformer provides simple closed-form design equations. The design is verified by simulation in Agilent ADS. For experimental verification a PCB prototype is fabricated using FR-4 material, operating at 1.45 GHz and 2.61 GHz. A good result is obtained confirming the theory and simulation.

1. INTRODUCTION

Impedance matching network is one of the ubiquitous blocks of many RF/Microwave circuits/systems such as amplifiers, mixers, oscillators, antennas and power dividers/combiners. Conventionally, quarter-wavelength/single-/double-stub impedance transformers have been used for this purpose [1]. However, such techniques face challenges in the design of dual-band/multi-band circuits and systems [2–5]. For instance, in the context of a typical dual-band amplifier, shown in Figure 1(a), the key challenge is to come up with appropriate matching networks so that they are able to work at two distinct frequencies [4, 6, 7].

Earlier reported distributed designs such as dual-band Chebyshev impedance transformer [10, 11], dual frequency transformer [9] and two-section 1/3-wavelength transmission line based transformer [8] are extremely useful for matching real load and source impedances. However, these designs are not able to provide matching when the load impedances are complex and frequency-dependent as is the case with a generic dual-band amplifier where the transistor may possess two different complex impedances (Z_L) at two different frequencies as depicted in Figure 1(b). There have been reports of matching two arbitrary complex load impedances to real source impedance based on two section impedance transformer [12–14] but again, they are not useful for situations where the complex load impedances are frequency-dependent. Reported design techniques [15–17] based around three section impedance transformers address this problem to some extent, but are either too complex to design or are extremely limited in frequency coverage.

Transmission line section loaded with stepped or open/short stubs [18], T-section network [19], dual-band line with different characteristic impedances [20] and Pi-section in conjunction with shunt-stub [21] are also commonly used for dual-band impedance transformation in the design of dual-band amplifiers. Usually lumped component based matching networks [22] are simpler, but fabrication of lumped component is difficult at higher frequencies and maintaining their value over a wide frequency range is extremely difficult [23]. Furthermore, few coupled line based dual-band impedance transformers

Received 4 September 2014, Accepted 12 October 2014, Scheduled 16 October 2014

* Corresponding author: Mohammad A. Maktoomi (ayatullahm@iiitd.ac.in).

[1] Wireless Systems Lab, Department of Electronics and Communications Engineering, IIIT Delhi, New Delhi 110020, India. [2] iRadio Lab, Department of Electrical and Computer Engineering, Schulich School of Engineering, University of Calgary, Calgary, Alberta T2N 1N4, Canada.

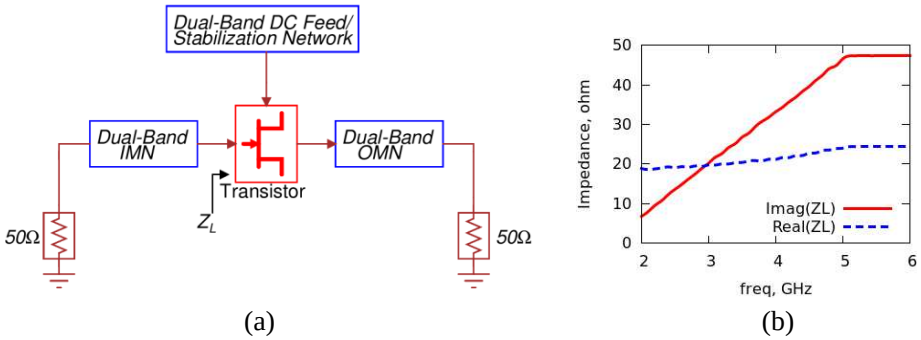

Figure 1. (a) Typical depiction of a dual-band RF amplifier, (b) frequency-dependent complex input impedance of a generic transistor (showing its real and imaginary parts).

exhibiting good performance have been reported and in general they may or may not provide inherently DC blocking [24–26].

In this paper, a simple dual-band impedance transformation technique is presented, which is capable of matching frequency-dependent complex load impedance at two distinct frequencies with real source impedance. The design utilizes coupled-line to modify one of the arms of a standard T-shaped network to achieve dual-band functionality. This modification allows simpler closed form solution for the design and also provides an additional feature of inherent DC blocking. The details of the proposed matching network are described in Section 2, while simulation and experimental results are discussed in Section 3 whereas conclusion is presented in Section 4.

2. PROPOSED IMPEDANCE TRANSFORMER

The proposed impedance matching network comprises three sections as shown in Figure 2. Z_s is the source side impedance whereas Z_L is the frequency-dependent load impedance. Section A consists of a transmission line section having characteristic impedance Z_1 and electrical length θ_1, while section B consists of a coupled-line having even/odd-mode impedances equal to Z_e and Z_o and electrical length θ_2 whereas section C is an open/short stub with characteristic impedance Z_3 and electrical length θ_3. All these electrical lengths are defined at first frequency f_1. The physical dimensions l (length), w (width) and s (separation between coupled lines) of various transmission-lines are also depicted in the figure. The respective admittances (impedances) looking into sections A, B and C are $Y_{in1}(Z_{in1})$, $Y_{in2}(Z_{in2})$

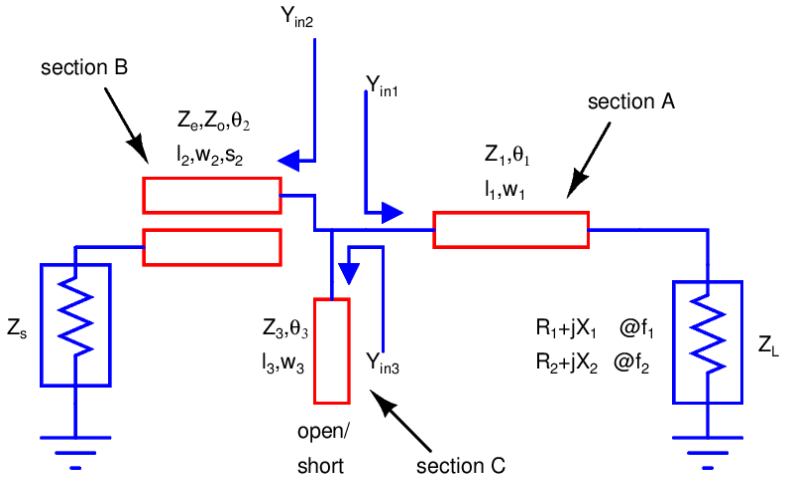

Figure 2. Proposed dual-band matching network.

and $Y_{in3}(Z_{in3})$. In this architecture, overall idea is to first match the real part of Y_{in1} to the real part of Y_{in2}, and then cancel out the 'leftover' imaginary part of $Y_{in1} + Y_{in2}$ by the shunt stub Y_{in3}.

2.1. Design of Section A

It is assumed that the load impedance at two arbitrary frequencies f_1 and f_2 are as follows:

$$Z_L|_{f_1} = R_1 + jX_1 \quad \text{and} \quad Z_L|_{f_2} = R_2 + jX_2.$$

As reported in [16], if section A is designed such that:

$$Z_1 = \sqrt{R_1R_2 + X_1X_2 + \frac{X_1 + X_2}{R_2 - R_1}(R_1X_2 - R_2X_1)} \tag{1a}$$

$$\theta_1 = \frac{p\pi + \arctan\left(\dfrac{Z_1(R_1 - R_2)}{R_1X_2 - R_2X_1}\right)}{1 + r}, \quad \text{where: } p \in I,\ r = f_2/f_1 \text{ with } r \geq 1 \tag{1b}$$

then the impedance looking into section A are complex conjugate of each other at the two frequencies, i.e., $Z_{in1}|_{f_1} = Z^*_{in1}|_{f_2}$, i.e., $Z_{in1} = 1/Y_{in1} = R_{in1} + jX_{in1}@f_1$ and $Z_{in1} = 1/Y_{in1} = R_{in1} - jX_{in1}@f_2$ where, the values of R_{in1} and X_{in1} are given by [14]:

$$R_{in1} = \frac{R_1Z_1^2\left[1 + \tan^2\theta_1\right]}{Z_1^2 - 2Z_1X_1\tan\theta_1 + \left(R_1^2 + X_1^2\right)\tan^2\theta_1} \tag{2a}$$

$$X_{in1} = \frac{\left(Z_1^2 - R_1^2 - X_1^2\right)Z_1\tan\theta_1 + Z_1^2X_1\left[1 - \tan^2\theta_1\right]}{Z_1^2 - 2Z_1X_1\tan\theta_1 + \left(R_1^2 + X_1^2\right)\tan^2\theta_1} \tag{2b}$$

Alternatively, Y_{in1} may also be obtained by inverting and rationalizing Z_{in1}:

$$Y_{in1} = G_1 - jB_1@f_1 \tag{2c}$$

$$Y_{in1} = G_1 + jB_1@f_2 \tag{2d}$$

where,

$$G_1 = R_{in1}/\left(R_{in1}^2 + X_{in1}^2\right) \tag{2e}$$

$$B_1 = X_{in1}/\left(R_{in1}^2 + X_{in1}^2\right) \tag{2f}$$

2.2. Design of Section B

The objective of this section is to match the real part of Y_{in1} to the real part of Y_{in2}, without any concerns about matching of their imaginary parts. There are two ways to analyze this section. One is based on using somewhat ideal yet simple equations for the coupled line while the other one uses the concept of image impedance to arrive at exact solution. Each of these approaches is described in the following subsections.

2.2.1. Simplified Analysis of Section B

The input impedance, Z_{in2} looking into section B is expressed by coupled line model [27]:

$$Z_{in2} = 1/Y_{in2} = -jZ_s(1 - n^2)\cot\theta_2 + n^2Z_s \tag{3a}$$

where,

$$n = \frac{\rho - 1}{\rho + 1} \tag{3b}$$

$$\rho = Z_e/Z_o \tag{3c}$$

It can be observed in 3(a) that all the terms are frequency-independent except the cotangent term. Now, noting that

$$\cot(\theta_2) = -\cot(r\theta_2) \Rightarrow \cot(\theta_2) = \cot(\pi - r\theta_2)$$
$$\Rightarrow \theta_2 = \pi - r\theta_2 + q\pi, \quad q = 0, \pm1, \pm2, \ldots$$

Thus, it can be deduced that for $Z_{in2}|_{f_1} = Z^*_{in2}|_{f_2}$, θ_2 should satisfy:

$$\theta_2 = \frac{(1+q)\pi}{1+r}, \quad q \in I \tag{4}$$

Furthermore, 3(a) can be simplified to express Y_{in2} as:

$$Y_{in2} = M + jN \tag{5}$$

where,

$$M = \frac{n^2}{Z_s\left[n^4 + \left((1-n^2)\cot\theta_2\right)^2\right]} \tag{5a}$$

$$N = \frac{\left(1-n^2\right)\cot\theta_2}{Z_s\left[n^4 + \left((1-n^2)\cot\theta_2\right)^2\right]} \tag{5b}$$

Setting of $M = G_1$, i.e., $\mathrm{Re}(Y_{in2}) = \mathrm{Re}(Y_{in1})$, and then simplification yields the value of parameter n defined in Equation 3(b):

$$n = \sqrt{\frac{-b \pm \sqrt{b^2 - 4ac}}{2a}} \tag{6a}$$

where,

$$a = 1 + \cot^2\theta_2, \tag{6b}$$

$$b = -\left(\frac{1}{G_1 Z_s} + 2\cot^2\theta_2\right), \tag{6c}$$

$$c = \cot^2\theta_2. \tag{6d}$$

It should be kept in mind that the model of coupled line given by 3(a) is highly idealized one [27]. A more accurate model requires intensive mathematical analysis as described in the next sub-section.

2.2.2. Exact Analysis of Section B

Using method of the image impedance [1], it can be shown that the $ABCD$ parameters of section B may be expressed as follows:

$$\begin{bmatrix} A & B \\ C & D \end{bmatrix} = \begin{bmatrix} c_{11} & c_{12} \\ c_{21} & c_{22} \end{bmatrix}$$

where,

$$c_{11} = \frac{\rho+1}{\rho-1}\cos\theta_2 = c_{22} \tag{7a}$$

$$c_{12} = -\frac{j}{2}\left[\frac{4\rho Z_o}{\rho-1}\frac{\cos^2\theta_2}{\sin\theta_2} - (\rho-1)Z_o\sin\theta_2\right] \tag{7b}$$

$$c_{21} = j\frac{2}{(\rho-1)Z_o}\sin\theta_2 \tag{7c}$$

Now, using two-port network theory Y_{in2} may be written as:

$$Y_{in2} = \frac{c_{21}Z_s + c_{22}}{c_{11}Z_s + c_{12}} \tag{8}$$

Simplification of (7) and (8) results into a form of Y_{in2} which is same as in (5), but now with:

$$M = \frac{4Z_s\left(\rho-1\right)^2}{4\left[Z_s^2\left(\rho+1\right)^2 - 2\rho\left(\rho-1\right)^2 Z_o^2\right]\cos^2\theta_2 + \left(\rho-1\right)^4 Z_o^2\sin^2\theta_2 + 16\rho^2 Z_o^2\cos^4\theta_2/\sin^2\theta_2} \tag{9a}$$

$$N = \frac{\rho+1}{Z_o}\frac{\left[4Z_s^2 - \left(\rho-1\right)^2 Z_o^2\right]\sin(2\theta_2) + 8\rho Z_o^2\cos^3\theta_2/\sin\theta_2}{4\left[Z_s^2\left(\rho+1\right)^2 - 2\rho\left(\rho-1\right)^2 Z_o^2\right]\cos^2\theta_2 + \left(\rho-1\right)^4 Z_o^2\sin^2\theta_2 + 16\rho^2 Z_o^2\cos^4\theta_2/\sin^2\theta_2} \tag{9b}$$

It can be observed that $Z_{in2}|_{f_1} = Z^*_{in2}|_{f_2}$, if the value of θ_2 is given by (4). It follows from following observations:

i. In 9(a), only even powers of $\sin\theta_2$ and $\cos\theta_2$ ensures that the values of M will repeat with a period of π. In addition, due to their even power M will not change its sign as the frequency switches from f_1 to f_2.
ii. Numerator of 9(b) also has a period of π but the sign of N will change as the frequency switches from f_1 to f_2.

One can proceed further using either of the two options after invoking $\mathrm{Re}(Y_{in2}) = \mathrm{Re}(Y_{in1})$:

a. Assume Z_o to be a free variable and solve for ρ.
b. Assume ρ to be a free variable and solve for Z_o.

Option (a) leads to a complicated fourth order equation in ρ (and hence in n), while option (b) leads to a simple quadratic equation in Z_o (of the form $ax^2 - b = 0$). Therefore, the following value for Z_o is obtained using option (b):

$$Z_o = \sqrt{4Z_s \frac{\left[(\rho-1)^2/G_1\right] - Z_s(\rho+1)^2\cos^2\theta_2}{(\rho-1)^4\sin^2\theta_2 + 16\rho^2\cos^4\theta_2/\sin^2\theta_2 - 8\rho(\rho-1)^2\cos^2\theta_2}} \tag{10}$$

It is interesting to note that the coupled line used in [26] has to achieve match both for real as well as for the imaginary parts of Y_{in1} with that of Y_{in2}. It is not easy to achieve at two different frequencies, especially with microstrip coupled line having unequal even/odd mode phase velocities. In the proposed network, only real part of Y_{in1} needs to be matched to the real part of Y_{in2} while their leftover imaginary parts are cancelled by the shunt stub described in Section 2.3. It also helps in extending the range of load that could be matched.

2.3. Design of Section C

This section cancels the imaginary part of $Y_{in1} + Y_{in2}$, given by Expressions 11(a) and 11(b), at two different frequencies.

$$j\,\mathrm{Im}(Y_{in1} + Y_{in2}) = -j(B_1 - N) \quad @f_1 \tag{11a}$$
$$= j(B_1 - N) \quad @f_2 \tag{11b}$$

As mentioned earlier, section C could either be an open stub or a short stub. For open stub to work at two distinct frequencies, following set of equations must be satisfied:

$$-j\,\mathrm{Im}(Y_{in1} + Y_{in2})|_{f_1} = j(1/Z_3)\tan\theta_3 \tag{12a}$$
$$-j\,\mathrm{Im}(Y_{in1} + Y_{in2})|_{f_2} = j(1/Z_3)\tan(r\theta_3) \tag{12b}$$

The terms Z_3 and θ_3 can be determined by solving (11) and (12):

$$\theta_3 = \frac{(1+s)\pi}{1+r}, \quad s \in I \tag{13a}$$
$$Z_3 = \tan\theta_3/(B_1 - N) \tag{13b}$$

A short stub may be shown to work at two frequencies with design equations similar to those given by (13), except that tangent in 13(b) needs to be replaced by cotangent.

It is important to note that $\{p, q, s\} \in I$ and can be chosen any integer value, but usually they are set to zero to get smaller footprint on the board. Furthermore, stubs may not be realizable in some situations and in those cases other techniques to realize complex impedances can be employed [18, 20].

2.4. Design Steps

Design steps can be summarized as follows:

i. The values of Z_1 and θ_1 are evaluated using (1) from the given values of r, R_1, X_1, R_2, and X_2.

ii. Then R_{in1} and X_{in1} are determined using 2(a) and 2(b). Subsequently the values of G_1 and B_1 are calculated from 2(e) and 2(f).

iii. This step is for Y_{in2} and therefore depends whether one follows simplified or exact analysis of section B:
(a) Simplified Analysis Flow: Using (4) and (6), θ_2 and n are found. It can be observed from 3(b) that since n is to be less than unity; one of the two values of n obtained from (6) may need to be discarded. The value of ρ is calculated from the chosen value of n. Either of Z_e or Z_o can be assumed to be a free variable and then the other can be found. It is important to keep in mind to get their realizable values. It may be noted that due to the use of simplified model in this case, the final design may require tuning/optimization which is a commonly found feature of today's RF/Microwave CAD tools.
(b) Exact Analysis Flow: θ_2 is found using (4). A suitable value of ρ is assumed and Z_o is evaluated from (10). Once the value of ρ and Z_o are known, the value for Z_e can be found using 3(c). Since this is an exact method so ideally there is no need for tuning/optimization.

iv. To design section C, (13) is used to get θ_3 and Z_3. Once again 5(b) or 9(b) may be used for finding out the value of N depending upon whether simplified or exact analysis was adopted for section B.

3. SIMULATION AND EXPERIMENTAL VERIFICATION

To verify that the values of Y_{in2} are complex conjugate of each other at the two frequencies, a coupled line having $\rho = 3$ and $Z_o = 25\,\Omega$ is considered. It is also assumed that $f_1 = 1\,\text{GHz}$ and $Z_s = 50\,\Omega$. Simulations are performed for three values of f_2: 2 GHz, 3 GHz and 4 GHz which corresponds to $r = 2$, 3 and 4, respectively. It is evident from the resulting plots of Y_{in2} from a simulation performed in Agilent ADS that as shown in Figure 3 the real part remains the same and the imaginary part just changes its sign as the frequency switches from f_1 to f_2.

Next, Table 1 provides a comparison between the proposed design and the one reported in [26]. It can be noted that θ_c in [26] and θ_2 in this paper has the same meaning. In this table, calculations are shown for the exact analysis described in section B. It can be seen that the value of Z_o for the chosen specifications is negative for the design reported in [26] while the proposed design gives realizable values for various parameters.

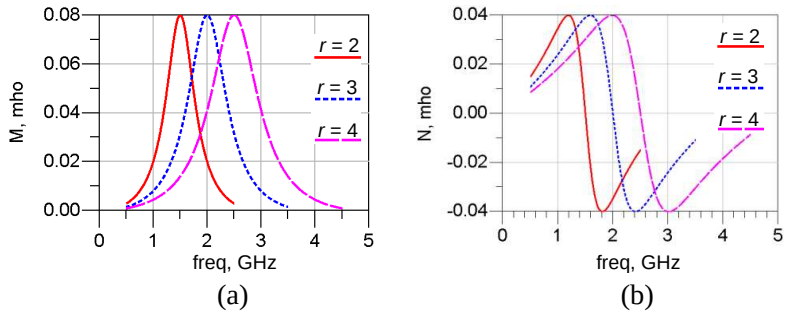

Figure 3. Variation of (a) real and (b) imaginary parts of Y_{in2} with frequency.

Table 1. Comparison with [26].

Ref.	Frequencies (GHz)	$Z_L(\Omega)$	Section A	Section B	Section C
[26]	$f_1 = 1.45$ $f_2 = 2.61$	$25 - j20$ $24.5 + j12.5$	$Z_1 = 111.36\,\Omega$ $\theta_1 = 1.42°$	$Z_o = -32.27\,\Omega$ $Z_e = 31.04\,\Omega$ $\theta_c = 64.29°$	NA
This Work				$\rho = 4$, $\theta_2 = 64.29°$ $Z_o = 29.16\,\Omega$ $Z_e = 116.64\,\Omega$	Open stub $Z_3 = 41.73\,\Omega$ $\theta_3 = 128.57°$

To further study the proposed matching network, an arbitrarily chosen frequency-dependent load is considered as depicted in Figure 4(a). The first frequency f_1 is fixed at 1 GHz and f_2 is swept as mentioned in Table 2. The load impedance along with the design parameters are also mentioned in Table 2 for five different cases. The simulated results for the designs listed in Table 2 are shown in Figure 4(b).

Further, a few more considered cases are given in Table 3. Here, the two frequencies are kept fixed and load impedances are made distinct. The simulated results for these designs in Table 3 are shown

Table 2. Design parameters for some cases where f_1 is fixed and f_2 is varying.

Case	Frequencies (GHz)	Z_L (Ω)	Section A	Section B	Section C
0	$f_1 = 1$ $f_2 = 1.7$	$70 + j10$ $73.5 + j14.48$	$Z_1 = 85.08\,\Omega$ $\theta_1 = 49.29°$	$\rho = 4$, $\theta_2 = 66.67°$ $Z_o = 68.63\,\Omega$ $Z_e = 274.52\,\Omega$	short stub $Z_3 = 136.25\,\Omega$ $\theta_3 = 133.34°$
1	$f_1 = 1$ $f_2 = 2$	$70 + j10$ $75 + j17$	$Z_1 = 88.29\,\Omega$ $\theta_1 = 44.96°$	$\rho = 2.2$, $\theta_2 = 60°$ $Z_o = 51\,\Omega$ $Z_e = 112.2\,\Omega$	open stub $Z_3 = 75.20\,\Omega$ $\theta_3 = 120°$
2	$f_1 = 1$ $f_2 = 2.5$	$70 + j10$ $77.5 + j23$	$Z_1 = 95.55\,\Omega$ $\theta_1 = 39.72°$	$\rho = 2.75$, $\theta_2 = 51.43°$ $Z_o = 35.71\,\Omega$ $Z_e = 98.20\,\Omega$	short stub $Z_3 = 39.85\,\Omega$ $\theta_3 = 51.43°$
3	$f_1 = 1$ $f_2 = 3$	$70 + j10$ $80 + j28$	$Z_1 = 101.43\,\Omega$ $\theta_1 = 34.71°$	$\rho = 3.5$, $\theta_2 = 45°$ $Z_o = 34.44\,\Omega$ $Z_e = 120.54\,\Omega$	short stub $Z_3 = 68.12\,\Omega$ $\theta_3 = 45°$
4	$f_1 = 1$ $f_2 = 3.5$	$70 + j10$ $82.5 + j35$	$Z_1 = 109.42\,\Omega$ $\theta_1 = 31.09°$	$\rho = 3.8$, $\theta_2 = 40°$ $Z_o = 22.67\,\Omega$ $Z_e = 86.15\,\Omega$	short stub $Z_3 = 107.60\,\Omega$ $\theta_3 = 120°$

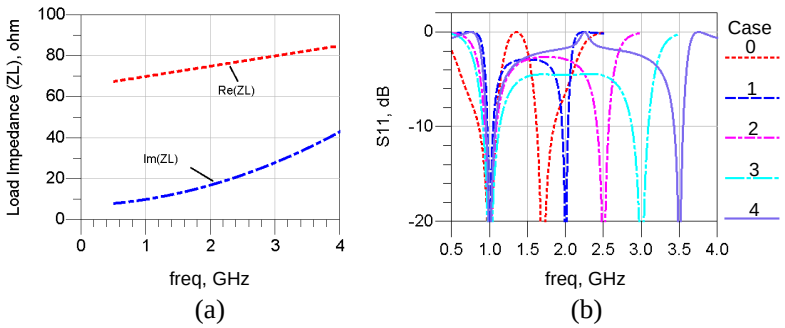

Figure 4. (a) Variation of real and imaginary parts of the frequency-dependent complex load (ZL), (b) S_{11} in dB for different cases listed in Table 2.

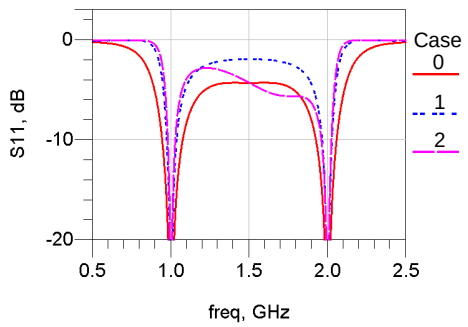

Figure 5. S_{11} in dB for different cases listed in Table 3.

Table 3. Design parameters for some cases where f_1 and f_2 are fixed and the load is varying.

Cases	Frequencies (GHz)	Z_L (Ω)	Section A	Section B	Section C
0	$f_1 = 1$ $f_2 = 2$	$30 - j27$ $47 + j60$	$Z_1 = 75.81\,\Omega$ $\theta_1 = 52.41^\circ$	$\rho = 2.5$, $\theta_2 = 60^\circ$ $Z_o = 57.52\,\Omega$ $Z_e = 143.8\,\Omega$	short stub $Z_3 = 88.67\,\Omega$ $\theta_3 = 60^\circ$
1		$80 + j15$ $90 + j24$	$Z_1 = 98.91\,\Omega$ $\theta_1 = 39.98^\circ$	$\rho = 2.1$, $\theta_2 = 60^\circ$ $Z_o = 48.06\,\Omega$ $Z_e = 100.93\,\Omega$	open stub $Z_3 = 69.46\,\Omega$ $\theta_3 = 120^\circ$
2		$50 + j60$ $20 - j30$	$Z_1 = 43.59\,\Omega$ $\theta_1 = 51.39^\circ$	$\rho = 2.1$, $\theta_2 = 60^\circ$ $Z_o = 53.53\,\Omega$ $Z_e = 112.4\,\Omega$	open stub $Z_3 = 49.94\,\Omega$ $\theta_3 = 120^\circ$

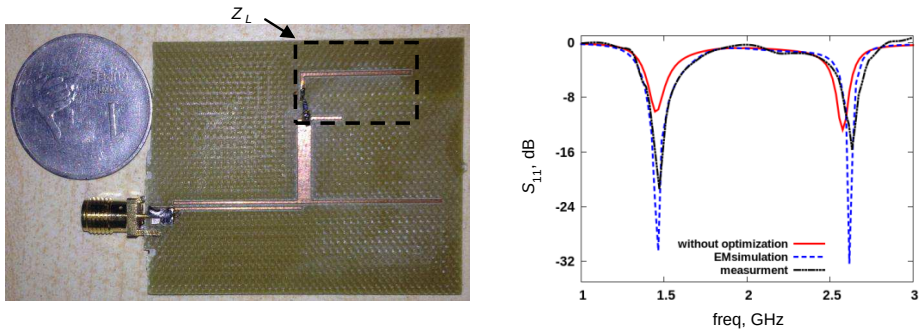

(a) (b)

Figure 6. (a) Photo of prototype manufactured in our lab and (b) plot of S_{11} in dB against frequency.

in Figure 5. All the above examples demonstrate the validity and usefulness of the proposed matching network.

Finally, the proposed matching network implemented on an FR-4 substrate ($\varepsilon_r = 4.7$, thickness = 1.5 mm) with 1 oz copper is shown in Figure 6(a). It is important to note that the designed prototype is based on simplified equations for section B and therefore extensive simulation and optimization in Agilent ADS were carried out. The physical dimensions of the implemented matching network are as follows (dimensions in mm): $l_1 = 13.91$, $l_2 = 21.66$, $l_3 = 21$, $w_1 = 2.25$, $w_2 = 0.64$, $w_3 = 0.76$ and $s_2 = 0.36$.

To verify the operation of the designed impedance transformer, a frequency-dependent load described in [26] is created. The load uses two open stubs and a Vishay-Dale CRCW series 10 Ω SMD resistor. The values of realized loads at the two frequencies $f_1 = 1.45$ GHz and $f_2 = 2.61$ GHz are as follows:

$$Z_L\,(\Omega) = \begin{cases} 8.049 - j26.868 & @f_1 \\ 114.621 + j190.247 & @f_2 \end{cases}$$

The simulated and measured results of the proposed matching network are shown in Figure 6(b). The plot of S_{11} in dB shows dips around the two design frequencies with the measured return loss of approximately 20.5 dB @ f_1 and 16 dB @ f_2. A slightly higher deviation is observed around f_2 perhaps due to the more pronounced impact of difference in even/odd-mode velocities. Nevertheless, it is evident from the plot that a well match can be obtained using the proposed circuit.

A comparison with some existing state of the art is shown in Table 4. It may be noted that since there is no standard definition for a frequency-dependent complex load; different reported designs have used different frequency dependency of load, thus it won't be fair to make comparison based on the bandwidth [28]. Moreover, the design reported in [25] also provides DC-blocking, but works for a very limited range of r.

Table 4. Comparison with some state of the art.

Ref. No.	Type of Load	Experiment	DC Blocking	Design Equations	Lumped/Distributed
9	Real	No	No	Simple	Distributed
10	Real	No	No	Simple	Distributed
13	Complex (but same @ f_1 & f_2)	No	No	Complex[2]	Distributed
16	FDCL[1]	No	No	Simple	Distributed
17	FDCL	Yes	No	Simple	Distributed
18	FDCL	Yes	No	Complex	Distributed
19	FDCL	No	No	Simple	Distributed
20	FDCL	Yes	No	Complex	Distributed
21	FDCL	Yes	No	Simple	Distributed
22	FDCL	No	No	Simple	Lumped
24	FDCL	Yes	No	Simple	Distributed
This Work	FDCL	Yes	Yes	Simple	Distributed

[1]FDCL: frequency-dependent complex load.
[2]Complex: requires computer to solve the design equations.

4. CONCLUSION

A new dual-band matching network utilizing modified T-section transmission line segment has been proposed in this paper. The new design can provide matching at two arbitrary frequencies for frequency-dependent complex loads. The design is unique in a way that only real part of Y_{in1} is required to match to the real part of Y_{in2} while their leftover imaginary parts are cancelled by a shunt stub. This enables the extending of the range of load that could be matched. The reported design also exhibits an interesting and useful characteristic of inherent DC blocking. The simulation and experimental results match well, thereby validate the design proposed in this paper.

REFERENCES

1. Pozar, D. M., *Microwave Engineering*, 3rd edition, John Wiley & Sons, New Delhi, 2010.
2. Rawat, K., M. S. Hashmi, and F. M. Ghannouchi, "Dual-band RF circuits and components for multi-standard software defined radios," *IEEE Circuits Syst. Mag.*, Vol. 12, No. 1, 12–32, First Quater 2012.
3. Kenington, P. B., *RF and Baseband Techniques for Software Defined Radio,* Artech House, Boston, 2005.
4. Hashemi, H. and A. Hajimiri, "Concurrent multiband low-noise amplifiers — Theory, design, and applications," *IEEE Trans. Microw. Theory Tech.*, Vol. 50, No. 1, 288–301, Jan. 2002.
5. Nallam, N. and S. Chatterjee, "Multi-band frequency transformations, matching networks and amplifiers," *IEEE Trans. Circuits Syst. I: Reg. Papers*, Vol. 60, No. 6, 1635–1647, Jun. 2013.
6. Iyer, B. and N. P. Pathak, "A concurrent dual-band LNA for noninvasive vital sign detection system," *Wiley Microw. & Opt. Tech. Lett.*, Vol. 56, No. 2, 391–394, Feb. 2014.
7. Rawat, K. and F. M. Ghannouchi, "Design methodology for dual-band doherty power amplifier with performance enhancement using dual-band offset lines," *IEEE Trans. Indust. Electronics*, Vol. 59, No. 12, 4831–4842, Dec. 2012.
8. Chow, Y. L. and K. L. Wan, "A transformer of one-third wavelength in two sections-for a frequency and its first harmonic," *IEEE Microw. Wireless Comp. Lett.*, Vol. 12, No. 1, 22–23, Jan. 2002.

9. Monzon, C., "A small dual-frequency transformer in two sections," *IEEE Trans. Microw. Theory Tech.*, Vol. 51, No. 4, 1157–1161, Apr. 2003.
10. Sophocles, J. and A. Orfanidis, "Two-section dual-band Chebyshev impedance transformer," *IEEE Microw. Wireless Comp. Lett.*, Vol. 13, No. 9, 382–384, Sep. 2003.
11. Castaldi, G., V. Fiumara, and I. Gallina, "An exact synthesis method for dual-band Chebyshev impedance transformers," *Progress In Electromagnetics Research*, Vol. 86, 305–319, 2008.
12. Colantonio, P., F. Giannini, and L. Scucchia, "A new approach to design matching networks with distributed elements," *15th International Conference on Microwaves, Radar and Wireless Communications, MIKON-2004*, Vol. 3, 811–814, 2004.
13. Wu, Y., Y. Liu, and S. Li, "A dual-frequency transformer for complex impedances with two unequal sections," *IEEE Microw. Wireless Comp. Lett.*, Vol. 19, No. 2, 77–79, Feb. 2009.
14. Dutta Roy, S. C., "Comment on 'a dual-frequency transformer for complex impedances with two unequal sections'," *IEEE Microw. Wireless Comp. Lett.*, Vol. 19, No. 9, 602, Sep. 2009.
15. Giannini, F. and L. Scucchia, "A complete class of harmonic matching networks: Synthesis and application," *IEEE Trans. Microw. Theory Tech.*, Vol. 57, No. 3, 612–619, Mar. 2009.
16. Liu, X., Y. Liu, S. Li, F. Wu, and Y. Wu, "A three-section dual-band transformer for frequency-dependent complex load impedance," *IEEE Microw. Wireless Comp. Lett.*, Vol. 19, No. 10, 611–613, Oct. 2009.
17. Wu, Y., Y. Liu, S. Li, C. Yu, and X. Liu, "A generalized dual-frequency transformer for two arbitrary complex frequency-dependent impedances," *IEEE Microw. Wireless Comp. Lett.*, Vol. 19, No. 12, 792–794, Dec. 2009.
18. Chuang, M.-L., "Dual-band impedance transformer using two-section shunt stubs," *IEEE Trans. Microw. Theory Tech.*, Vol. 58, No. 5, 1257–1263, May 2010.
19. Nikravan, M. A. and Z. Atlasbaf, "T-section dual-band impedance transformer for frequency-dependent complex impedance loads," *Electronics Letters*, Vol. 47, No. 9, 551–553, Apr. 28, 2011.
20. Rawat, K. and F. M. Ghannouchi, "Dual-band matching technique based on dual-characteristic impedance transformers for dual-band power amplifiers design," *IET Microwaves, Antennas & Propagation*, Vol. 5, No. 14, 1720–1729, Nov. 18, 2011.
21. Zheng, X., Y. Liu, S. Li, C. Yu, Z. Wang, and J. Li, "A dual-band impedance transformer using Pi-section structure for frequency-dependent complex loads," *Progress In Electromagnetics Research C*, Vol. 32, 11–26, 2012.
22. Moon, B.-T. and N.-H. Myung, "A dual-band impedance transforming technique with lumped elements for frequency-dependent complex loads," *Progress In Electromagnetics Research*, Vol. 136, 123–139, 2013.
23. Hsieh, K.-A., H.-S. Wu, K.-H. Tsai, and C.-K. C. Tzuang, "A dual-band 10/24-GHz amplifier design incorporating dual-frequency complex load matching," *IEEE Trans. Microw. Theory Tech.*, Vol. 60, No. 6, 1649–1657, Jun. 2012.
24. Wu, Y., W. Sun, S.-W. Leung, Y. Diao, and K.-H. Chan, "A novel compact dual-frequency coupled-line transformer with simple analytical design equations for frequency-dependent complex load impedance," *Progress In Electromagnetics Research*, Vol. 134, 47–62, 2013.
25. Li, S., B. Tang, Y. Liu, S. Li, C. Yu, and Y. Wu, "Miniaturized dual-band matching technique based on coupled-line transformer for dual-band power amplifiers design," *Progress In Electromagnetics Research*, Vol. 131, 195–210, 2012.
26. Wu, Y., Y. Liu, S. Li, and C. Yu, "New coupled-line dual-band DC-block transformer for arbitrary complex frequency-dependent load impedance," *Wiley Microw. & Opt. Tech. Lett.*, Vol. 54, No. 1, 139–142, Jan. 2012.
27. Mongia, R. K., I. J. Bahl, P. Bhartia, and J. Hong, *RF and Microwave Coupled Line Circuits,* 2nd Edition, Chapter 12, Artech House, Norwood, 2007.
28. Liu, Y., Y. Zhao, S. Liu, Y. Zhou, and Y. Chen, "Multi-frequency impedance transformers for frequency-dependent complex loads," *IEEE Trans. Microw. Theory Tech.*, Vol. 61, No. 9, 3225–3235, Sep. 2013.